

**Fermi-Surface Measurements of Mixed-Valence CeSn<sub>3</sub>**

W. R. Johanson and G. W. Crabtree

*Argonne National Laboratory, Argonne, Illinois 60439*

and

A. S. Edelstein<sup>(a)</sup>*University of Illinois at Chicago Circle, Chicago, Illinois 60680, and Argonne National Laboratory, Argonne, Illinois 60439*

and

O. D. McMasters

*Ames Laboratory, Iowa State University, Ames, Iowa 50011*

(Received 5 November 1980)

The first measurements of Fermi-surface properties in a mixed-valence metal with use of the de Haas-van Alphen effect are presented. At least nine separate frequency branches in CeSn<sub>3</sub> are seen and effective masses as large as 9.2 have been measured. The experiments show that hybridization between the conduction states and local *f* states occurs coherently in the mixed-valence compound CeSn<sub>3</sub>, resulting in Bloch states with well-defined wave vector and energy.

PACS numbers: 71.25.Hc, 71.70.Ms

Mixed-valence behavior has been examined by a variety of experimental methods, including magnetic susceptibility, lattice constant, Mössbauer effect, x-ray-photoemission spectroscopy, and neutron scattering measurements. Nearly all of these experiments focus on the mixed-valence ion or its interaction with the lattice. An equally important interaction occurs between the mixed-valence ion and the conduction electrons. However, the properties of conduction electrons in mixed-valence materials have received relatively little attention, primarily because of the lack of experiments which cleanly separate the conduction-electron behavior from that of the localized electrons.

In this report we present the first results of de Haas-van Alphen (dHvA) measurements on a mixed-valence material. The dHvA effect is sensitive only to properties of the conduction electrons and gives detailed information on Fermi-surface geometry, cyclotron effective masses, and energy width of the Landau levels. Unlike many of the other experiments, the dHvA effect occurs in thermodynamic equilibrium so that its observation does not upset the electronic structure of the local or itinerant states. Our experiment is the first to show conclusively that the *f* electrons in CeSn<sub>3</sub> (and probably other mixed-valence metals) must be treated by an itinerant-electron rather than a localized-electron picture. Our data provide the means for a detailed test of band-theory-based models of mixed valence in

CeSn<sub>3</sub>.

The mixed-valence metal CeSn<sub>3</sub> has been extensively studied by lattice constant,<sup>1</sup> thermal expansion,<sup>1,2</sup> magnetic susceptibility,<sup>3-5</sup> elastic constant,<sup>6</sup> and neutron scattering<sup>7</sup> measurements. The susceptibility is Curie-Weiss-like at high temperature, becomes approximately temperature independent at intermediate temperatures with a broad maximum near 140 K, and increases sharply below 40 K in a sample-dependent way. These and other properties have been interpreted phenomenologically<sup>3</sup> in terms of a characteristic temperature in the range 135-190 K, well above the temperatures where the present dHvA experiments were performed.

Crystals of CeSn<sub>3</sub> were prepared in tungsten crucible from high-purity starting materials by using the Bridgman technique.<sup>8</sup> Two dHvA samples in the shape of 1-mm-edge cubes were spark cut from one of the as-grown crystals (resistance ratio ~250) and electropolished by using a perchloric-acid-methanol solution to protect the surface from deterioration. The dHvA oscillations were measured in fields up to 15 T and at temperatures between 0.3 and 1.12 K with use of the field modulation technique. Details of the cryostat design and experimental procedure are published elsewhere.<sup>9</sup>

dHvA data were taken in CeSn<sub>3</sub> for the field direction in two different planes: The (110) plane and a nonsymmetry plane passing approximately through  $\langle 001 \rangle$  and a point 8° from  $\langle 110 \rangle$  in the

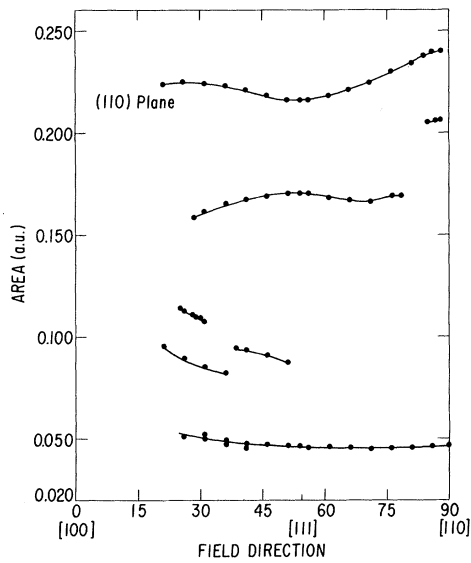


FIG. 1. Extremal-cross-sectional-area measurements in  $\text{CeSn}_3$  in the (110) plane. Several small-area branches below 0.02 a.u. observed in this crystal are not shown.

(001) plane. The cross-sectional areas as a function of field direction in these two planes are shown in Figs. 1 and 2. We see many low-area branches below 0.01 a.u. and a smaller number of higher branches with area up to  $\sim 0.24$  a.u. For comparison, the area of the (100) Brillouin-zone face is 0.495 a.u., implying that the surfaces we observe account for a sizable fraction of the zone volume. The low-area branches appear to be continuous across the entire plane, suggesting several small closed sheets of surface. (In Fig. 2, we do not show data for these branches for angles less than  $17^\circ$  because the signals were weak because of an unfavorable orientation of the pickup coil relative to the crystal for this sample. These branches were seen near  $\langle 100 \rangle$  in the other sample.) In principle, the crossings and splittings of these branches determine where in the zone these closed sheets are located, but the resolution in area of our present data is not good enough to make a unique interpretation. The temperature and field dependence of the amplitudes suggest that some of these small orbits have low effective masses, and the volume contained in the largest of the associated sheets accounts for less than 0.005 electron per unit cell. Therefore, these sheets contribute insignificantly to the density of states and the number of conduction electrons.

The area branches above 0.02 a.u. were care-

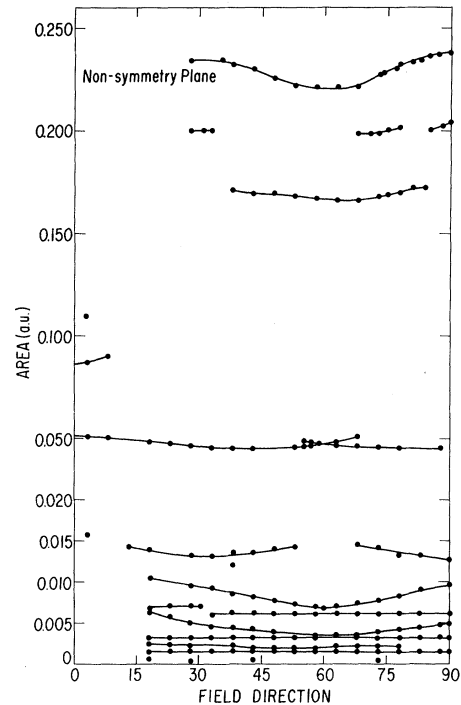


FIG. 2. Extremal-cross-sectional-area measurements in  $\text{CeSn}_3$  in a nonsymmetry plane.  $0^\circ$  on the horizontal scale is near  $\langle 001 \rangle$ ;  $90^\circ$  is near a point  $8^\circ$  from  $\langle 110 \rangle$  in the (001) plane. Note the change in vertical scale at 0.02 a.u. Data for the small-area branches below 0.02 a.u. at angles less than  $17^\circ$  are not shown because the signals were weak because of an unfavorable orientation of the pickup coil relative to the crystal for this sample.

fully studied in both the (110) and the nonsymmetry planes. In the (110) plane, none of these branches is observed at all angles, which is normally interpreted as implying an open Fermi surface. However, in the case of  $\text{CeSn}_3$  the surface could still be closed with the signal disappearing for a range of angles if the effective mass becomes large or if the crystal is strained. Evidence for either of these possibilities can be found in the measured masses and Dingle temperatures (see Table I), both of which attain large values and show considerable anisotropy near certain angles. The branches occurring at 0.24, 0.15, and 0.05 a.u. exist over much of the (110) and the nonsymmetry planes, and we take them to be the most important orbits on the large sheets of the surface. The observation of extrema rather than crossings at  $\langle 111 \rangle$  and the absence of splitting in the nonsymmetry plane for the two largest branches indicates that they may be centered at  $\Gamma$  or  $R$ , but not at  $X$  or  $M$ . The

TABLE I. Effective masses ( $m^*/m$ ) and Dingle temperatures ( $X$ ) in CeSn<sub>3</sub>. For the nonsymmetry plane, 0° is near  $\langle 001 \rangle$  and 90° is approximately 8° from  $\langle 110 \rangle$  in the (001) plane. For the symmetry plane, 0° is along  $\langle 100 \rangle$ .

Plane	Angle (deg.)	Area (a.u.)	$m^*/m$	$X$ (K)
Nonsymmetry	68	0.046	4.6	
	68	0.166	9.2	
	68	0.221	4.6	
(110)	70	0.045	4.6	0.12
	46	0.168	6.0	0.4
	46	0.218	4.2	1.5
	54	0.216	4.4	0.85

branch at 0.05 a.u. appears to split in the nonsymmetry plane near 60° suggesting that it is not centered at  $\Gamma$  or  $R$ . The short angular range of the branch at 0.20 a.u. near 90° in both planes suggests that it is either a noncentral orbit on a closed sheet or a symmetry-centered orbit on an open sheet. The short branches at  $\sim 0.1$  a.u. and 35° in the (110) plane and at  $\sim 0.2$  a.u. and 30° and 70° in the nonsymmetry plane do not appear in both planes and we interpret them as noncentral orbits. Preliminary band-structure calculations<sup>10</sup> predicting closed convoluted surfaces at  $\Gamma$  and  $R$  offer some support for our interpretations. However, we will not discuss these calculations here because we wish to emphasize the general implications of the experimental results rather than their relation to any specific model.

The effective-mass and Dingle-temperature measurements are summarized in Table I. All of the large-area orbits have high effective masses, ranging from 4.4 to 9.2. There is one indication of strong anisotropy on the branch at  $\sim 0.15$  a.u., where the mass changes from 6.0 to 9.2 in going from the (110) plane to the nonsymmetry plane. These high effective-mass values are consistent with the large electronic specific heat of CeSn<sub>3</sub>,<sup>5,11</sup>  $13.3 \pm 2.5$  mJ/K<sup>2</sup> · mole-atom. This may be compared with the value 9.45 mJ/K<sup>2</sup> · mole-atom for Pd,<sup>12</sup> which has measured effective masses<sup>13</sup> on its two largest sheets in the range 2–8, values comparable to but lower than those observed in CeSn<sub>3</sub>. We interpret the high specific heat and effective masses in CeSn<sub>3</sub> as evidence for a large admixture of the conduction states with  $f$  states. These high-mass orbits must be associated with the mixed-valence behavior.

CeSn<sub>3</sub> has Fermi-surface properties consider-

ably different from those of its non-mixed-valence analog LaSn<sub>3</sub>. In measurements to fields of 7 T, we find<sup>14</sup> that the pattern of orbital areas in LaSn<sub>3</sub> is quite different from that of CeSn<sub>3</sub>, implying qualitative differences in the Fermi-surface geometries for the two metals. The comparison of effective masses is especially striking: All of the measured masses in LaSn<sub>3</sub> are less than unity. These low masses approximately scale with the electronic specific heat<sup>15,16</sup> of LaSn<sub>3</sub>,  $\gamma = 2.7$  mJ/K<sup>2</sup> · mole-atom.

The observation of dHvA oscillations in CeSn<sub>3</sub> provides new insight into the behavior of mixed-valence systems and suggests new directions for further work. The high effective masses which we observe over much of the Fermi surface show explicitly that the Ce  $f$  electron hybridizes with conduction-band states and not with some other local state on the Ce ion. Further, the existence of well-defined dHvA oscillations with reasonably low Dingle temperatures associated with these hybridized states is direct evidence for the coherent nature of the mixed-valence state in CeSn<sub>3</sub>. Our results imply that the hybridization of the  $f$  electron with the conduction states at all Ce sites must be correlated so that Bloch states of definite energy and wave vector are formed. This correlation among sites is incompatible with "impurity" models of mixed valence which consider each site to hybridize independently to form a broad virtual bound state about the mixed-valence ion. Such a state cannot propagate through the lattice nor will it permit the observation of the dHvA effect. The low-temperature coherence which we observe in CeSn<sub>3</sub> is consistent with the small residual resistivity in this<sup>17</sup> and other unstable moment systems<sup>18,19</sup> and we expect it to be a general feature of mixed valence in stoichiometric ordered compounds.

The observation of coherent hybridized Bloch states in CeSn<sub>3</sub> strongly supports an itinerant picture of mixed valence. The high effective masses which we observe on all the large-area orbits and the significant differences between the LaSn<sub>3</sub> and CeSn<sub>3</sub> Fermi-surface geometries indicate that  $f$  electron hybridization strongly affects most, if not all, of the conduction-band states at the Fermi energy. As these states determine many of the physical properties of the metal, we may reasonably expect that much mixed-valence behavior can be explained in terms of the itinerant-electron picture. Such an approach naturally explains the approximate scaling of the effective masses and electronic-specific-heat values in

LaSn<sub>3</sub>, CeSn<sub>3</sub>, and transition metals like Pd.

One of the most important outstanding issues in the itinerant-electron picture is the importance of narrow-band correlation effects. Our results make possible for the first time a quantitative exploration of this question through comparison of the experimental Fermi-surface geometry and effective masses with those of careful band-theory calculations of CeSn<sub>3</sub> and LaSn<sub>3</sub>. Such calculations are in progress<sup>10</sup> but are not yet far enough advanced to provide definitive conclusions.

Experimentally, our work establishes a new probe of mixed valence in ordered metallic systems. Fermi-surface geometry and effective masses are both quite sensitive to the hybridization process and offer a potentially rich source of both qualitative and quantitative information on how the *f*-electron and conduction-band states combine to form hybridized energy bands. As itinerant models of mixed valence are developed, experimental Fermi-surface information will provide the best detailed test of their validity.

We have enjoyed many useful and stimulating discussions with Dr. D. D. Koelling and Dr. S. K. Sinha. This work was supported by the U. S. Department of Energy and by the Director of Energy Research, Office of Basic Energy Sciences, Contract No. WPAS-KC-0201. Ames Laboratory is operated for the U. S. Department of Energy by Iowa State University under Contract No. W-7405-ENG-82.

<sup>(a)</sup>Present address: Energy Conversion Devices, Inc., Troy, Mich. 48084.

<sup>1</sup>I. R. Harris and G. V. Raynor, *J. Less-Common Met.*

*9*, 7 (1965).

<sup>2</sup>E. Umlauf, P. Sutsch, and E. Hess, *Crystalline Electric Field and Structural Effects in f-Electron Systems* (Plenum, New York, 1980), p. 341.

<sup>3</sup>J. M. Lawrence, *Phys. Rev. B* **9**, 3770 (1979).

<sup>4</sup>T. Tsuchida and W. E. Wallace, *J. Chem. Phys.* **43**, 3811 (1965).

<sup>5</sup>J. R. Cooper, C. Rizzuto, and G. Olcese, *J. Phys. (Paris), Colloq.* **32**, C1-1136 (1971).

<sup>6</sup>A. S. Edelstein, S. K. Sengupta, R. L. Carlin, and O. D. McMasters, *Solid State Commun.* **34**, 781 (1980).

<sup>7</sup>C. Stassis, C. K. Loong, B. N. Harmon, S. J. Liu, and R. M. Moon, *J. Appl. Phys.* **50**, 7567 (1979).

<sup>8</sup>C. Stassis, C.-K. Loong, J. Zarestky, O. D. McMasters, and R. M. Nicklow, to be published.

<sup>9</sup>D. P. Karim, J. B. Ketterson, and G. W. Crabtree, *J. Low Temp. Phys.* **30**, 389 (1978).

<sup>10</sup>D. D. Koelling, unpublished.

<sup>11</sup>R. A. Elenbaas, C. J. Schinkel, and C. J. M. van Deudekom, *J. Magn. Magn. Mater.* **15-18**, 979 (1980).

<sup>12</sup>B. M. Boerstal, J. J. Zwart, and J. Hansen, *Physica (Utrecht)* **54**, 442 (1971).

<sup>13</sup>D. H. Dye, S. A. Campbell, G. W. Crabtree, J. B. Ketterson, N. B. Sandesara, and J. J. Vuillemin, *Phys. Rev. B* **23**, 462 (1981).

<sup>14</sup>W. R. Johanson, G. W. Crabtree, D. D. Koelling, A. S. Edelstein, and O. D. McMasters, *Bull. Am. Phys. Soc.* **25**, 344 (1980).

<sup>15</sup>E. Bucher, K. Andres, J. P. Maita, and G. W. Hull, *Helv. Phys. Acta* **41**, 723 (1968).

<sup>16</sup>M. H. Van Maaren and E. E. Havinga, in *Proceedings of Low Temperature Physics, LT-13, 1972* (Plenum, New York, 1974), p. 392.

<sup>17</sup>B. Stalinski, Z. Kletowski, and Z. Henkie, *Phys. Status Solidi* **19**, K165 (1973).

<sup>18</sup>A. S. Edelstein, C. J. Tranchita, O. D. McMasters, and K. A. Gschneidner, *Solid State Commun.* **15**, 81 (1974).

<sup>19</sup>A. S. Edelstein, R. E. Majewski, and T. H. Blewitt, *Solid State Commun.* **23**, 593 (1977).